



The anti-ALS drug riluzole attenuates pericyte loss in the diabetic retinopathy of streptozotocin-treated mice



Jeong A. Choi^{a,1}, Yoo-Ri Chung^{b,1,2}, Hye-Ran Byun^{a,3}, Hwangseo Park^d,
Jae-Young Koh^{a,c,*}, Young Hee Yoon^{b,*}

^a Neural Injury Research Center, Asan Institute for Life Sciences, University of Ulsan College of Medicine, Seoul, Republic of Korea

^b Department of Ophthalmology, University of Ulsan College of Medicine, Seoul, Republic of Korea

^c Department of Neurology, Asan Medical Center, University of Ulsan College of Medicine, Seoul, Republic of Korea

^d Department of Bioscience and Biotechnology, Sejong University, Seoul, Republic of Korea

ARTICLE INFO

Article history:

Received 13 July 2016

Revised 24 November 2016

Accepted 5 December 2016

Available online 8 December 2016

Keywords:

Diabetic retinopathy

Pericyte

Protein kinase C

Riluzole

ABSTRACT

Loss of pericytes, considered an early hallmark of diabetic retinopathy, is thought to involve abnormal activation of protein kinase C (PKC). We previously showed that the anti-amyotrophic lateral sclerosis (ALS) drug riluzole functions as a PKC inhibitor. Here, we examined the effects of riluzole on pathological changes in diabetic retinopathy. Pathological endpoints examined *in vivo* included the number of pericytes and integrity of retinal vessels in streptozotocin (STZ)-induced diabetic mice. In addition, PKC activation and the induction of monocyte chemoattractant protein (MCP1) were assessed in diabetic mice and in human retinal pericytes exposed to advanced glycation end product (AGE) or modified low-density lipoprotein (mLDL). The diameter of retinal vessels and the number of pericytes were severely reduced, and the levels of MCP1 and PKC were increased in STZ-induced diabetic mice. Administration of riluzole reversed all of these changes. Furthermore, the increased expression of MCP1 in AGE- or mLDL-treated cultured retinal pericytes was inhibited by treatment with riluzole or the PKC inhibitor GF109203X. *In silico* modeling showed that riluzole fits well within the catalytic pocket of PKC. Taken together, our results demonstrate that riluzole attenuates both MCP1 induction and pericyte loss in diabetic retinopathy, likely through its direct inhibitory effect on PKC.

© 2016 Published by Elsevier Inc.

1. Introduction

Diabetic retinopathy (DR), a retinal microvascular disease, is one of the leading causes of severe visual loss among the working-age population (Praidou et al., 2010; Yau et al., 2012; Bandello et al., 2013; Ruta et al., 2013). DR is a multifactorial disease whose pathogenesis remains incompletely understood. Nearly all patients of type 1 diabetes and more

than 60% of patients with type 2 diabetes suffers of some degree of DR around 15–20 years after diagnosis (Williams et al., 2004). DR can be broadly divided into two clinical stages: nonproliferative DR (NPDR) and proliferative DR (PDR). During the NPDR phase, abnormal permeability and/or nonperfusion of retinal capillaries result in the earliest visible sign of retinal damage followed by the formation of microaneurysms (Williams et al., 2004). In PDR, proliferation of new but fragile blood vessels on the retinal surface (neovascularization) is the hallmark finding (Williams et al., 2004). Among newly diagnosed patients with type 2 diabetes, 22% with no DR at baseline developed NPDR at 6 years and 29% of patients with baseline DR showed progression of DR of two or more steps on the Early Treatment Diabetic Retinopathy Study scale after 6 years' disease duration (Williams et al., 2004). Streptozotocin (STZ)-induced diabetic mice typically present features of NPDR, while oxygen-induced retinopathy mouse models and Kimba (trVEGF029) transgenic mouse models are commonly used to investigate PDR (Lai and Lo, 2013).

An early event in DR that occurs prior to the development of microaneurysm formation or neovascularization is the breakdown of the blood-retinal barrier (BRB), leading to the increased permeability of retinal capillaries followed by the increased secretion of

Abbreviations: AGE, advanced glycation end products; BRB, blood-retinal barrier; BSA, bovine serum albumin; DR, diabetic retinopathy; FBS, fetal bovine serum; FITC, fluorescein isothiocyanate; mLDL, modified low-density lipoprotein; MCP1, monocyte chemoattractant protein-1; NPDR, nonproliferative diabetic retinopathy; PBS, phosphate-buffered saline; PDGF, platelet-derived growth factor; PDGFR- β , platelet-derived growth factor receptor- β ; PDR, proliferative diabetic retinopathy; PKC, protein kinase C; STZ, streptozotocin; VEGF, vascular endothelial growth factor.

* Corresponding authors at: 88, Olympic-ro 43-Gil, Songpa-gu, Seoul 138-736, Republic of Korea.

E-mail addresses: jkho@amc.seoul.kr (J.-Y. Koh), yhyoon@amc.seoul.kr (Y.H. Yoon).

¹ These authors equally contributed to this work.

² Present address: Department of Ophthalmology, Ajou University School of Medicine, Suwon, Republic of Korea.

³ Present address: Department of Integrative Biology and Physiology, University of California Los Angeles, CA, USA.

inflammatory cytokines (Kaur et al., 2008; Praidou et al., 2010; Chew et al., 2014). The functional abnormalities and eventual loss of pericytes may play a critical role in this process (Praidou et al., 2010; Fu et al., 2012; Du et al., 2013; Lai and Lo, 2013). Hyperglycemia per se may directly lead to vasoregression, or it may do so indirectly via the action of advanced glycation end products (AGEs), which are non-enzymatically formed in a hyperglycemic environment (Chen et al., 2006; Singh et al., 2014; Cai and McGinnis, 2016). Modified low-density lipoprotein (mLDL) is also formed in diabetic patients through oxidation and/or glycation, and is known to cause accelerated vascular changes in diabetes (Sonoki et al., 2002; Renier et al., 2003; Zhang et al., 2008). The decrease in pericyte numbers is associated with a subsequent increase in vascular permeability, decrease in perfusion, and induction of angiogenic factors such as vascular endothelial growth factor (VEGF) (Motiejunaite and Kazlauskas, 2008; Praidou et al., 2010).

Protein kinase C (PKC) plays a key role in VEGF signaling, and aberrant PKC signaling, specifically that of the PKC β isoenzyme, is thought to be involved in the pathogenesis of DR (Aiello, 2002; Budhiraja and Singh, 2008; Praidou et al., 2010). Accordingly, PKC β has recently been suggested as a potential target in the treatment of both early and late diabetic vascular complications (Aiello, 2002; Menne et al., 2013; Koya, 2014). Other factors that have been causally linked to DR, including inflammatory cytokines such as monocyte chemoattractant protein-1 (MCP1), are also modulated by the PKC pathway (Kim et al., 2012). We have previously found that riluzole, the FDA-approved drug for amyotrophic lateral sclerosis (ALS), is an inhibitor of PKC β , showing that riluzole attenuates pathological changes in oxygen-induced retinopathy, a surrogate model of DR (Sims, 1986). Since PKC is involved in the early stage of disease progression (Sims, 1986; Noh et al., 2000), these findings suggest the possibility that riluzole might also have an inhibitory effect on DR.

Commonly used streptozotocin (STZ) or alloxan-induced rodent models exhibit rapid onset of hyperglycemia and several symptoms of NPDR such as retinal pericyte loss and capillaries, thickening of vascular basement membrane, and increased vascular permeability (Cai and McGinnis, 2016). Apoptosis of retinal ganglion cells and vascular cells can be identified since 6 weeks of hyperglycemia (Lai and Lo, 2013), while retinal pericyte loss starts between 4 and 8 weeks of diabetes (Hammes, 2005). Accordingly, in the present study, we examined the effects of riluzole on the induction of cytokines in STZ-induced diabetic mice and by putative mediators of DR in cultured human retinal pericytes.

2. Methods

2.1. Chemicals

STZ, dimethyl sulfoxide (DMSO), riluzole, and GF109203X were purchased from Sigma (St. Louis, MO, USA). GF109203X, a pan-PKC inhibitor, was selected as positive control. AGE was purchased from Bio Vision (Milpitas, CA, USA). mLDL was prepared by diluting low-density lipoprotein, obtained from Calbiochem (La Jolla, CA, USA), in phosphate-buffered saline (PBS) and incubating with 10 μ M CuCl₂ at 37 °C for 24 h (Jenkins et al., 2000; Lyons et al., 2000).

2.2. Animals

The animal experimental protocol was approved by the Internal Review Board for Animal Experiments of Asan Life Science Institute, University of Ulsan College of Medicine (Seoul, Korea). The animals were treated in accordance with the Guide for the Care and Use of Laboratory Animals as adopted and promulgated by the U.S. National Institutes of Health. Male, 8-week-old (22–25 g) C57BL/6NcrSlc mice were obtained from Japan SLC, Inc. (Hamamatsu, Japan) and maintained at 24 °C \pm 0.5 °C under a 12-hour light/dark cycle. Animals were injected intraperitoneally with STZ (150 mg/kg body weight in 50 mM

citrate buffer, pH 4.5) or citrate buffer alone (control) after 4 h of fasting (Lai and Lo, 2013; Leskova et al., 2013). Diabetes was confirmed using Super Glucocard II from Dongbang International Inc. (Seoul, Korea), and animals with blood glucose levels higher than 300 mg/dl 1 week after STZ injection were considered to be diabetic. This is one of the standard protocols recommended by the Animal Models of Diabetic Complications Consortium (Lai and Lo, 2013). Mice were injected intraperitoneally with riluzole (1 mg/kg body weight per day) or 1% DMSO in saline daily for 4 weeks. The number of mice used for experimental setup and treatment is described in Table S1.

2.3. Human retinal pericyte culture

A human retinal pericyte cell line was obtained from Applied Cell Biology Research Institute (Kirkland, WA, USA) and cultured in Dulbecco's Modified Eagle's Medium with 1 g/l glucose (Invitrogen, Carlsbad, CA, USA), supplemented with 10% fetal bovine serum (FBS; Invitrogen), 1% penicillin-streptomycin (Lonza, Allendale, NJ, USA), and 2 mM glutamine (Sigma) at 37 °C in a humidified 5% CO₂ incubator. Cells between passage 5 and 10 were used for experiments after reaching approximately 80% confluence.

2.4. Fluorescein angiography

Eight weeks after STZ injection, mice were anesthetized by isoflurane (1.5%) inhalation, and fluorescein angiography was performed using a MICRON III retinal imaging system (Phoenix Research Laboratories, Inc., Pleasanton, CA, USA). Photographs were obtained using a mouse-specific contact lens in MICRON III after intraperitoneal injection of 0.2 ml of 2% fluorescein sodium (Alcon Laboratories, Inc., Fort Worth, TX, USA) (Choi et al., 2013). Fluorescein angiographs of the early phase were taken at 3 min after fluorescein injection, while those of the late phase were taken at 15 min. Quantification of fluorescence was evaluated as follows: fluorescein intensity was measured at regular distances from the optic disc between major retinal vessels by Image J software (NIH, Bethesda, MD, USA), and 5 measurements of intensity were averaged for each eye.

2.5. Fluorescein isothiocyanate (FITC) staining of retinal flat-mounts

All mice were injected intramuscularly with 0.3 ml of Zoletil (diluted 1:5), and cardiac perfusion was performed with 0.5 ml of 15 mg/ml dextran (2000 kDa, #FD2000S, Sigma) in saline. After 5 min, eyes were fixed in 4% paraformaldehyde for 1 h at room temperature and transferred to a culture dish filled with PBS. Retinal tissues were dissected and flat-mounted on slides with coverslips. Capillary intensity was measured as the fluorescein intensity of capillaries by Image J software, and 5 measurements of capillary intensity were averaged for each retina.

2.6. Immunohistochemistry

The presence of pericytes was assessed by immunostaining retinal tissues with an antibody against platelet-derived growth factor receptor- β (PDGFR- β , 1:100; #ab32570, Epitomics, Burlingame, CA, USA). Co-staining with CD31 antibody (1:500, #MAB1398Z, Millipore, MA, USA), an endothelial cell marker, was performed to verify the presence of retinal vessels, while Hoechst 33342 (1:5000, #H3570, Molecular Probes™, MA, USA) was also used to confirm the loss of cells. After fixing in 4% paraformaldehyde, retinas were washed in PBS and incubated in a permeabilizing and blocking solution consisting of PBS containing 0.2% Triton X-100 and 1% bovine serum albumin (BSA). After incubation with a primary antibody at 4 °C for 7 days, tissues were washed in PBS three times for 10 min. They were further incubated with Alexa Fluor-conjugated secondary antibodies at 4 °C for 1 day (1:500; Alexa Fluor 555-donkey anti-rabbit IgG or Alexa Fluor 647-goat anti-hamster IgG, Invitrogen). After incubation with a secondary antibody, tissues were

stained with Hoechst 33342 in PBS for 10 min and then washed in PBS three times for 10 min. Stained retinal tissues were flat-mounted with DAKO (#S3023, DAKO, Denmark) on glass slides. Confocal images were obtained by confocal microscopy (LSM710, Carl-Zeiss, Oberkochen, Germany).

2.7. Western blot analysis

Human retinal pericyte cells and retinal tissues were lysed in RIPA buffer (20 mM Tris-Cl pH 7.4, 150 mM NaCl, 1 mM EDTA, 1 mM EGTA, 1% Triton X-100, 2.5 mM sodium pyrophosphate, 1 μ M Na₃VO₄, 1 μ g/ml leupeptin, and 1 mM phenylmethylsulfonyl fluoride). The lysates were centrifuged, and the protein concentration in supernatants was determined using the DC Protein Assay Reagent (Bio-Rad, Hercules, CA, USA). Samples containing equal amounts of protein were separated by sodium dodecyl sulfate-polyacrylamide gel electrophoresis (SDS-PAGE) and then transferred to polyvinylidene difluoride membranes (Millipore, Billerica, MA, USA). Membranes were incubated overnight at 4 °C with anti-MCP1 (1:1000; #NBP1-07035, NOVUS), anti-pPKC (1:1000; #9371S, Cell Signaling, Beverly, MA, USA), and/or anti- β -actin (1:2500; #A5060, Sigma) primary antibodies, followed by incubation with horseradish peroxidase-conjugated goat anti-rabbit IgG (1:10,000; Pierce, Rockford, IL, USA).

2.8. ELISA for MCP1

After reaching 80% confluence, human retinal pericytes in 24-well plates were exposed to 500 μ g/ml AGE or 100 μ g/ml mLDL for 24 or 12 h, respectively. Cells were co-treated with riluzole (15 μ M); GF109203X (2.5 μ M) was used as a positive control for PKC inhibition.

Cell supernatants containing most soluble proteins were centrifuged and collected for ELISA. MCP1 protein levels in supernatants were determined using an ELISA kit (R&D Systems, Minneapolis, MN, USA).

2.9. Immunocytochemistry

Human retinal pericyte cells were plated on glass slides and exposed to either 500 μ g/ml AGE or 100 μ g/ml mLDL for 24 or 12 h respectively, with or without co-treatment with 15 μ M riluzole or 2.5 μ M GF109203X. Cells were then fixed in 4% paraformaldehyde for 1 h, permeabilized, and blocked by incubating with PBS/0.2% Triton X-100/1% BSA for 30 min. After incubation with anti-MCP1 primary antibody (1:500; #NBP1-07035, NOVUS) at 4 °C overnight, cells were incubated with Alexa Fluor-conjugated secondary antibodies (1:1000; Alexa Fluor 555-donkey anti-rabbit IgG, Invitrogen), mounted with mounting media, and examined by confocal microscopy (LSM710, Carl-Zeiss).

2.10. Docking simulations

Three-dimensional (3D) atomic coordinates of PKC were prepared from the corresponding X-ray crystal structure in complex with a potent inhibitor (PDB code: 3IW4) (Wagner et al., 2009), used as the receptor model for docking simulations with riluzole and GF109203X. Gasteiger-Marsilli atomic charges were assigned to all protein and ligand atoms to calculate the electrostatic interaction in the PKC-riluzole complex (Gasteiger and Marsili, 1980). Docking simulations were then carried out with the AutoDock program (Morris et al., 1998) to obtain the binding mode of riluzole in the ATP-binding site of PKC. Of the 20 conformations of riluzole generated from docking simulations, those that clustered together had similar binding modes, differing by <1.5 Å in positional root-mean-square deviation. The most stable binding configuration in the top-ranked cluster was selected for further analysis.

2.11. Statistical analysis

All results are presented as means \pm SEM. Student's *t*-tests were used to evaluate the significance of difference between two groups. *P*-values < 0.05 were considered significant. All statistical analyses and graphical presentations were conducted and created using Sigma Plot version 10.0 software.

3. Results

3.1. STZ-induced DR in mice

Retinal vascular changes in live mice were examined 8 weeks after the injection of STZ using fundus photography and fluorescein angiography. Compared with angiographic images from age-matched controls that underwent vehicle injections, images of STZ-treated mouse eyes were blurrier, reflecting increased leakage of fluorescein, especially at the late stage (after 15 min) (Fig. 1A). Quantification of the relative fluorescence in the areas between retinal arteries confirmed these findings, showing that fluorescein leakage was significantly increased in the eyes of STZ-treated mice compared with those of controls (Fig. 1B). Hence, STZ-treatment successfully produced DR in mice.

3.2. Hypoperfusion and pericyte loss in STZ-induced diabetic mice

To examine the chronological changes of the retinal vasculature in DR, we prepared retinal flat mounts from control and STZ-treated mice at 2-week intervals from 4 to 10 weeks after injection. Pathological vascular changes are reported to be diverse even within the same species of chemically induced diabetic animal models (Cai and McGinnis, 2016), while there are studies reporting pericyte loss and vascular leakage being detected between 4 and 8 weeks of diabetes (Hammes, 2005; Lai and Lo, 2013). Fluorescein leakage was noted even at 4 weeks, and became more severe at 6 weeks in our experiment protocols. At 8 and 10 weeks, fluorescein in vessels was markedly reduced, likely signifying vessel obliteration and hypoperfusion (Fig. 2A). Additionally, retinal vascular diameters were also reduced at 8 weeks after STZ injection compared to control mice (Fig. S3).

To examine the loss of pericytes, we immunostained retinal pericytes with an antibody against the pericyte marker, PDGFR- β . Consistent with previous results (Hammes, 2005; Kim et al., 2012), we found a marked reduction in the number of pericytes at the same time that hypoperfusion became evident (8 and 10 weeks) (Fig. 2B). Counts of pericytes over total cells in retinal flat mounts confirmed that the loss of pericytes became significant at 8 weeks, and further progressed at 10 weeks after STZ-treatment (Fig. 2C, D).

3.3. Alteration of MCP1 expression by AGE and mLDL in cultured retinal pericytes

Various cytokines may contribute to the progression of DR. One such cytokine is MCP1, which is present in vitreous humor and serum, and contributes to the degree of membrane proliferation in proliferative DR (Panee, 2012). Several factors have been proposed to induce MCP1 in retinal cells in the context of diabetes, including hyperglycemia per se, AGE and mLDL, probably through PKC activation (Eisma et al., 2015). To address the mechanism of MCP1 induction, we treated cultured retinal pericytes with AGE or mLDL, in the presence and absence of riluzole or the pan-PKC inhibitor GF109203X, and examined MCP1 expression by Western blotting, ELISA, and immunocytochemistry.

Treatment of pericytes with 500 μ g/ml AGE increased the levels of phosphorylated PKC and induced an increase in the expression of MCP1. Both PKC activation and induction of MCP1 expression by AGE were completely blocked by addition of GF109203X (2.5 μ M), indicating that MCP1 induction was dependent on PKC activation (Fig. 3A–C). Consistent with its reported PKC inhibitory properties, riluzole also blocked

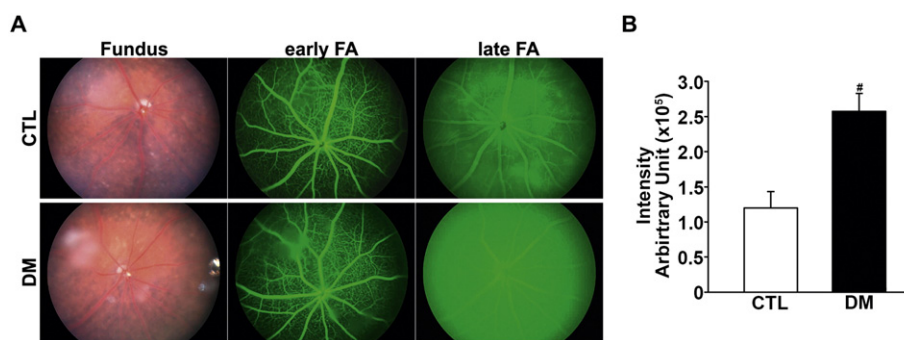


Fig. 1. Fundus fluorescein angiography of DR. (A) Representative photographs of fluorescein angiography (FA) taken 8 weeks after STZ injection showed more prominent fluorescein leakage at late stage in diabetic mice ($n = 14$) compared to control mice ($n = 10$). (B) Quantification of fluorescein angiography results ($\#P < 0.005$). Fluorescein angiographs of the early phase were obtained 3 min after fluorescein injection while those of the late phase were taken at 15 min. The intensity of fluorescein leakage was quantified as the difference between intensities of late phase and early phase and averaged from 5 different measurements.

AGE effects on PKC and MCP1 (Fig. 3A–C). Immunocytochemistry and ELISA confirmed that AGE markedly increased MCP1 levels, and riluzole attenuated these effects (Fig. 3D, E). Similar increases in PKC activity and MCP1 expression were also induced by mLDL; again, these effects were completely abrogated by the addition of riluzole or GF109203X (Fig. 3F–J).

3.4. *In vivo* effect of riluzole on MCP1 induction in DR

Having observed an inhibitory effect of riluzole on AGE- and mLDL-induced MCP1 expression in cultured pericytes, we next examined riluzole effects on STZ-induced DR in mice. To determine whether riluzole affected glucose metabolism per se, we measured body weights and blood glucose levels weekly during the experiment. Neither parameter was significantly different between vehicle and riluzole treatment in control or STZ-treated diabetic mice (Fig. 4). All STZ-treated mice exhibited profound hyperglycemia during this period (Fig. 4B).

After 4 weeks of riluzole treatment, intracellular levels of MCP1 in retinas were examined by Western blot analysis. As shown in Fig. 5(B, C), the level of MCP1 in retinas was approximately doubled in diabetic mice. As was the case in cultured pericytes, administration of riluzole completely blocked the increased MCP1 induction in retinas of diabetic mice (Fig. 5B, C).

3.5. Attenuation of STZ-induced DR by riluzole

Fluorescein angiography confirmed that treatment with riluzole significantly decreased leakage in STZ-induced diabetic mice (Fig. 6A, B). Also, the hypoperfused area was reduced and capillary density was attenuated in riluzole-treated diabetic mice compared to untreated diabetic mice (Fig. 6C, D). Immunostaining with PDGFR- β antibody and co-staining with CD31 antibody showed loss of retinal pericytes in retinal capillaries in non-treated diabetic mice and this was protected in riluzole-treated mice (Fig. 6E, F). Reduced retinal vascular diameters were also recovered with riluzole treatment (Fig. S3).

3.6. *In silico* binding analysis of riluzole with respect to PKC β

Although we have shown that riluzole is a PKC inhibitor in cells and in isolated membrane fractions (Noh et al., 2000), it has not yet been determined whether it directly interacts with PKC. To examine the possibility of direct binding of riluzole to PKC, we performed docking simulations of riluzole in the ATP-binding site of PKC. The lowest-energy conformation of riluzole in the ATP-binding site of PKC is shown in Fig. 7(A). Both riluzole and GF109203X appear to be stabilized in the unique binding pocket comprising the Gly loop and the hinge region of the ATP-binding site at the interface of the N- and C-terminal domains. As a check on the possibility of allosteric inhibition of PKC by

riluzole, we performed additional docking simulations with extended 3D grid maps to include the entire kinase domain. No peripheral binding pocket was found in which riluzole could be stabilized with a negative binding free energy. It is thus expected that the inhibitory activity of riluzole stems from its specific binding in the ATP-binding site of PKC.

We next turned to defining the detailed interactions responsible for the stabilization of riluzole in the ATP-binding pocket. Notably, the binding mode of riluzole computed by docking simulations, shown in Fig. 7(B), indicates that the terminal amino group of riluzole donates a hydrogen bond to the backbone aminocarbonyl oxygen of Glu418. This hydrogen bond is similar to that found to play an anchoring role in binding of a potent PKC inhibitor (Wagner et al., 2009), suggesting that the hydrogen-bond interactions with backbone groups of the hinge region are necessary for the inhibitory activity of riluzole. In the calculated PKC-riluzole complex, an additional hydrogen bond is established between the $-\text{CF}_3$ moiety and the side-chain butylammonium ion of Lys368. This hydrogen bond also seems to contribute significantly to the stabilization of riluzole in the ATP-binding pocket. Riluzole appears to be stabilized further in the ATP-binding site through the establishment of hydrophobic interactions between its nonpolar groups and the side chains of Phe350, Val353, Ala366, Leu391, Met417, and Ala480. Judging from the pattern of PKC-riluzole complex formation derived from docking simulations, the inhibitory activity of riluzole can be attributed to the two hydrogen bonds and the hydrophobic interactions established simultaneously in the ATP-binding pocket.

4. Discussion

The central finding of the present study is that riluzole, a FDA-approved anti-ALS drug, has beneficial effects on DR in mice treated with STZ. First, riluzole ameliorated pericyte loss, fluorescein leakage, and hypoperfusion in the retina of diabetic mice. Second, riluzole inhibited the induction of MCP1, a major inflammatory cytokine implicated in DR, in retinas of diabetic mice as well as in cultured pericytes treated with AGE or mLDL, which may contribute to the pathology of DR. At least *in vitro*, the effects of riluzole were mimicked by GF109203X, a standard pan-PKC inhibitor, consistent with the interpretation that riluzole effects are mediated by PKC inhibition.

DR is one of the leading causes of blindness in adults, afflicting about 35% of diabetic patients during their lifetime (Yau et al., 2012; Ruta et al., 2013). The pathogenesis of DR is not yet fully understood (Praidou et al., 2010; Abcouwer, 2013; Chew et al., 2014), although hyperglycemia-induced changes in inflammatory cytokines, microvascularity, and angiogenic factors are likely involved (Witmer et al., 2003; Bhagat et al., 2009; Bandello et al., 2013; Tarr et al., 2013). The microvascular dysfunction in DR clinically encompasses capillary hyperpermeability and obliteration, which results in complications such as diabetic macular edema and

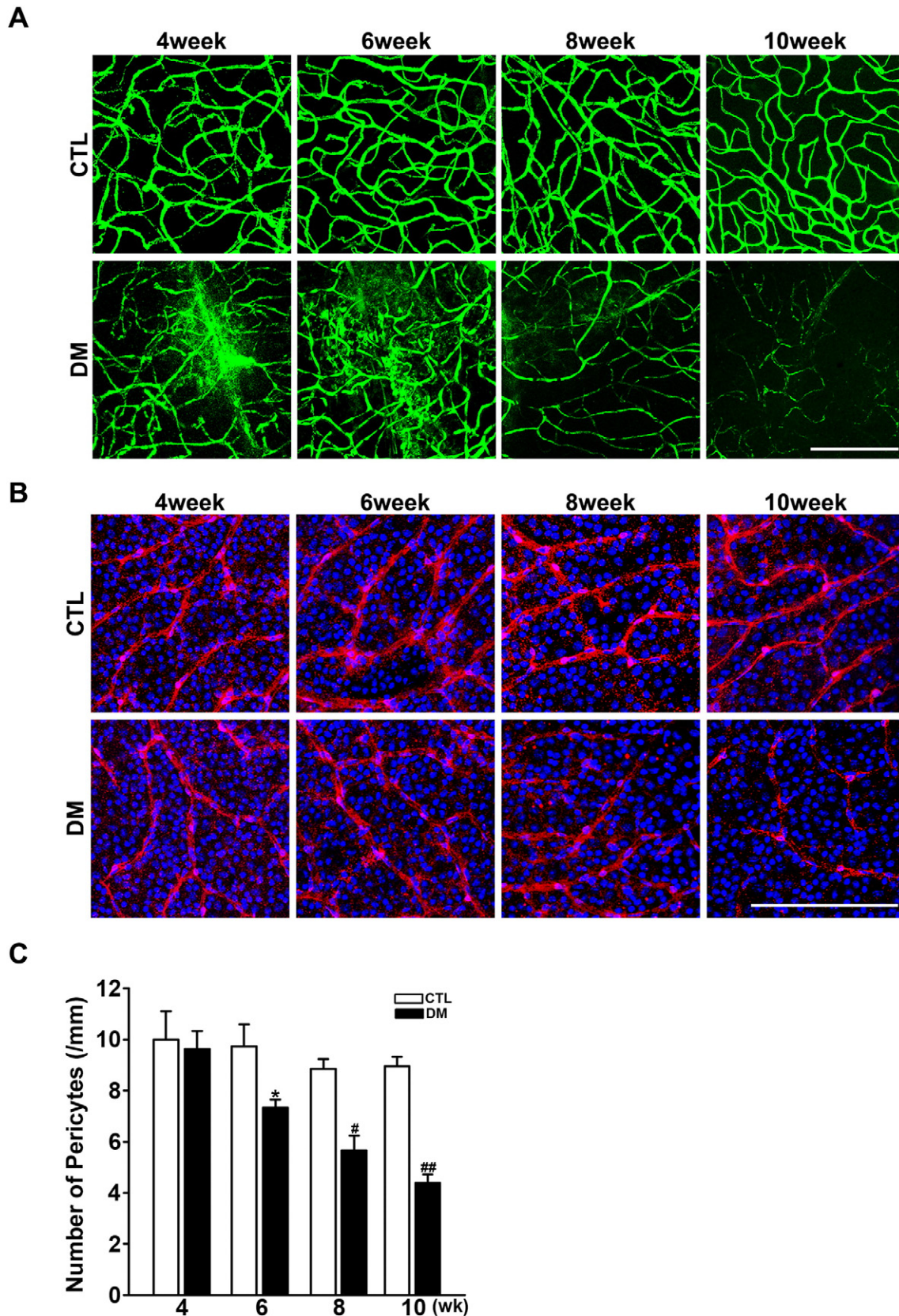


Fig. 2. Hypoperfusion and pericyte loss in diabetic mice. (A) Hypoperfusion in DR. Leakage was evident after 4 weeks of diabetes induction, and the hypoperfused area had expanded at 8 weeks (green: FITC-dextran). (B) Pericyte loss in DR. Immunostaining of retinal flat mounts was performed with antibodies for PDGFR- β (red) and Hoechst (blue). The number of pericytes decreased in diabetic mice beginning at 8 weeks, and was half that of controls at 10 weeks (4, 6, 8, 10 weeks; CTL $n = 2$, DM $n = 3$). Original magnification, $\times 200$; scale bar, 200 μm . (C) Quantification of pericytes cells per retinal vascular area (number/mm²). * $P < 0.05$, # $P < 0.005$, ## $P < 0.001$).

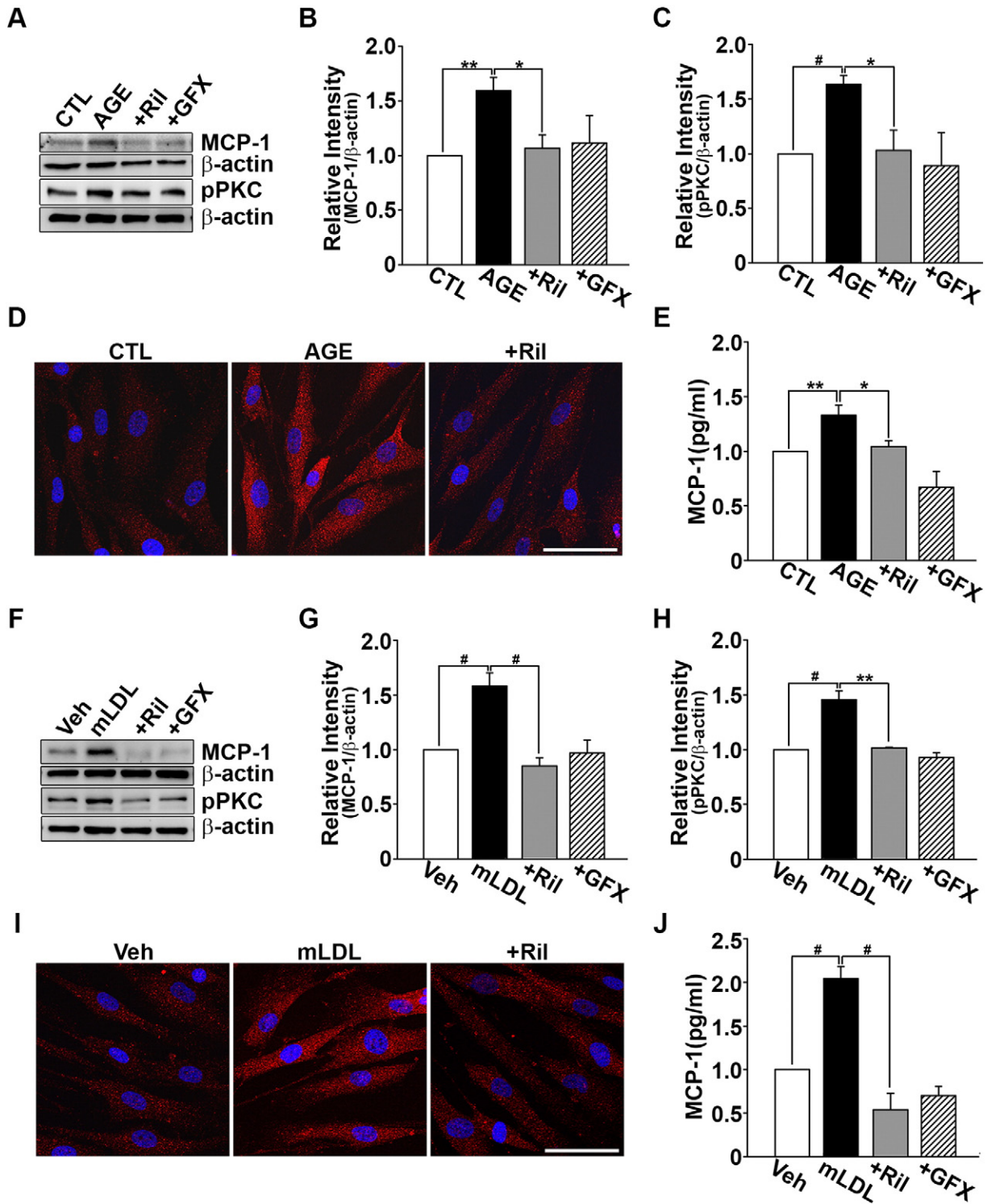


Fig. 3. AGE- and mLDL-induced MCP1 expression and its attenuation by riluzole in human cultured retinal pericytes. Treatment with AGE (500 μ g/ml) or mLDL (100 μ g/ml) increased intracellular MCP1 levels, and this was attenuated by GF109203X (2.5 μ M) or riluzole (15 μ M). (A) Western blot analysis of AGE-induced MCP1 expression and PKC activation in the presence and absence of riluzole. Quantification of western blot of MCP1 expression (B, $n = 3$) and PKC activation (C, $n = 3$). AGE-induced increases in MCP1 levels in the presence and absence of riluzole determined by immunohistochemistry (D) and ELISA (E). (F) Western blot analysis of mLDL-induced MCP1 expression and PKC activation in the presence and absence of riluzole. Quantification of western blot of MCP1 expression (G, $n = 3$) and PKC activation (H, $n = 3$). mLDL-induced increases in MCP1 levels in the presence and absence of riluzole determined by immunohistochemistry (I) and ELISA (J). ELISA and WB were performed with cell lysates. Original magnification, $\times 400$; scale bar, 100 μ m (* $P < 0.05$, ** $P < 0.01$, # $P < 0.005$).

retinal neovascularization (Bandello et al., 2013). Diabetic macular edema, caused by the disruption of the BRB, is a chronic vision-threatening complication that may occur at any stage of DR (Bhagat et al., 2009; Bandello et al., 2013). On the other hand, progressive retinal

hypoperfusion caused by the closure of capillaries results in induction of angiogenic factors such as VEGF. Thus, induced proliferative neovascularization, in turn, causes vitreous hemorrhage or tractional retinal detachment (LeCaire et al., 2013; Lutty, 2013). The mainstays of current

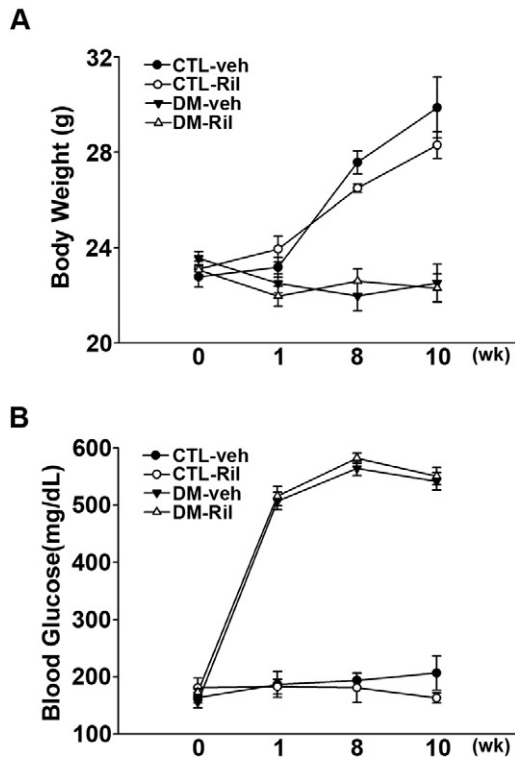


Fig. 4. Body weights and blood glucose levels in diabetic mice. There were no significant differences between riluzole and vehicle-treated groups in diabetic mice ($n = 29$ for DM-veh and $n = 31$ for DM-Ril) or controls ($n = 12$ for CTL-veh and $n = 10$ for CTL-Ril).

therapy for DR are surgery for vitreous hemorrhage and retinal detachment, and treatment with anti-angiogenic drugs, such as anti-VEGF monoclonal antibodies, VEGF receptor blockers or steroids, for macular edema and neovascularization (Praidou et al., 2010). However, these therapies are often started in only late stages of DR, and are designed to prevent further deterioration rather than restore impaired vision (Aiello, 2002).

The loss of pericytes may play a crucial initial role in all of the above pathological changes of DR. Pericytes are essential for the integrity and regulation of retinal capillaries by exerting smooth muscle-like actions. Likely reflecting this, retinal vessels are covered with pericytes at the highest density in the body (Sims, 1986; Motiejunaite and Kazlauskas, 2008). Notably, pericytes are especially enriched in the retina, highlighting their crucial role in this tissue (Motiejunaite and Kazlauskas, 2008; Du et al., 2013). Pericytes, as part of the neurovascular unit, are a major component

of the blood-brain barrier/BRB, assigned for vessel stabilization and neurovascular coupling (Troost et al., 2016). The loss of pericytes, which results in BRB disruption as well as reduced perfusion, is a characteristic pathologic feature of early-stage DR (Motiejunaite and Kazlauskas, 2008; Praidou et al., 2010; Fu et al., 2012). The accumulation of cytotoxic AGE in pericytes and decreases in PDGF levels have been suggested as possible causes of pericyte dropout in DR (Motiejunaite and Kazlauskas, 2008). Clinically, diabetic patients with late-stage DR exhibit diffuse leakage of fluorescein from hyperpermeable new retinal vessels on fluorescein angiography (Wu et al., 2013). In the current study, we verified the vascular leakage and loss of pericytes in STZ-induced diabetic mice using a mouse-specified fluorescein angiography imaging system and staining of retinal flat mounts (Leskova et al., 2013). We verified the role of AGE and mLDL, factors known to contribute to diabetic vascular complications, in the retinal pericytes, confirming previous reports that, among several tested diabetes-involved cytokines, these two factors in particular increase the induction of MCP1 (Friedman, 1999; Fu et al., 2012). MCP1 expression was also clearly increased in the retinas of diabetic mice, indicating that MCP1 is highly expressed in DR.

Hyperglycemia results in the generation of AGE and reactive oxygen species, which in turn leads to activation of the PKC pathway (Friedman, 1999; Aiello, 2002; Thallas-Bonke et al., 2008; Bandello et al., 2013). PKC acts as a key signaling mediator for many growth factors, neurotransmitters, and inflammatory cytokines (Aiello, 2002; Gerald and King, 2010). In DR, PKC increases vascular permeability and upregulates VEGF signaling, and thus is considered a potential therapeutic target in DR (Murakami et al., 2012; Bandello et al., 2013; Tarr et al., 2013). Riluzole, a FDA-approved drug for ALS, has been considered to be a pre-synaptically acting antigitamate drug (Kim et al., 2007). However, we have presented evidence that riluzole inhibits PKC (Sims, 1986; Noh et al., 2000). Thus, we hypothesized that riluzole may have beneficial effects in DR. Consistent with this idea, riluzole attenuated AGE- and mLDL-induced increases in pPKC levels and MCP1 expression in cultured pericytes as well as in diabetic mice. This effect of riluzole was similar to that of the pan-PKC inhibitor, GF109203X, which also reduced the levels of pPKC and MCP1, further supporting the idea that PKC inhibition underlies the mechanism of action of riluzole. The in vivo effects of riluzole are unlikely attributable to its effects on glucose metabolism, since blood glucose levels and body weights were not affected by riluzole treatment.

Increased vascular permeability and reduced perfusion are hallmark pathological features of DR. We used a mouse-tailored ocular imaging system, MICRON III, to visualize the induction of DR in live mice. In vivo fluorescein angiography showed differences in fluorescein leakage between control and riluzole-treated diabetic mice: whereas fluorescein leakage was a prominent feature in control diabetic mice, leakage was significantly decreased in riluzole-treated mice. Flat mount histology

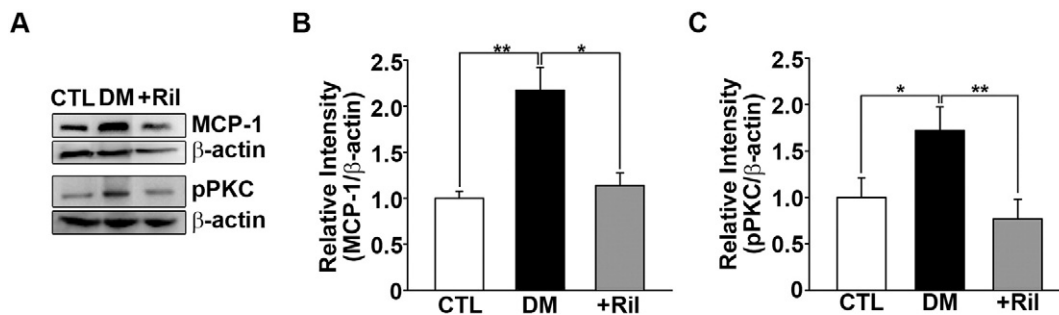


Fig. 5. Induction of MCP1 and pPKC and their attenuation by riluzole in retinal tissues of diabetic mice. (A) Western blot analysis of MCP1 and pPKC expression in eye tissues of control, riluzole (1 mg/kg)-treated, and untreated diabetic mice. (B, C) MCP1 and pPKC levels were significantly increased in diabetic mice ($n = 12$ for MCP1 and $n = 10$ for pPKC respectively) compared to controls ($n = 9$ respectively). MCP1 and pPKC levels were significantly reduced in diabetic mice treated with riluzole ($n = 10$ for MCP1 and $n = 11$ for pPKC respectively) compared with untreated diabetic mice (* $P < 0.05$, ** $P < 0.01$). Western blot was performed with whole eyeball lysates.

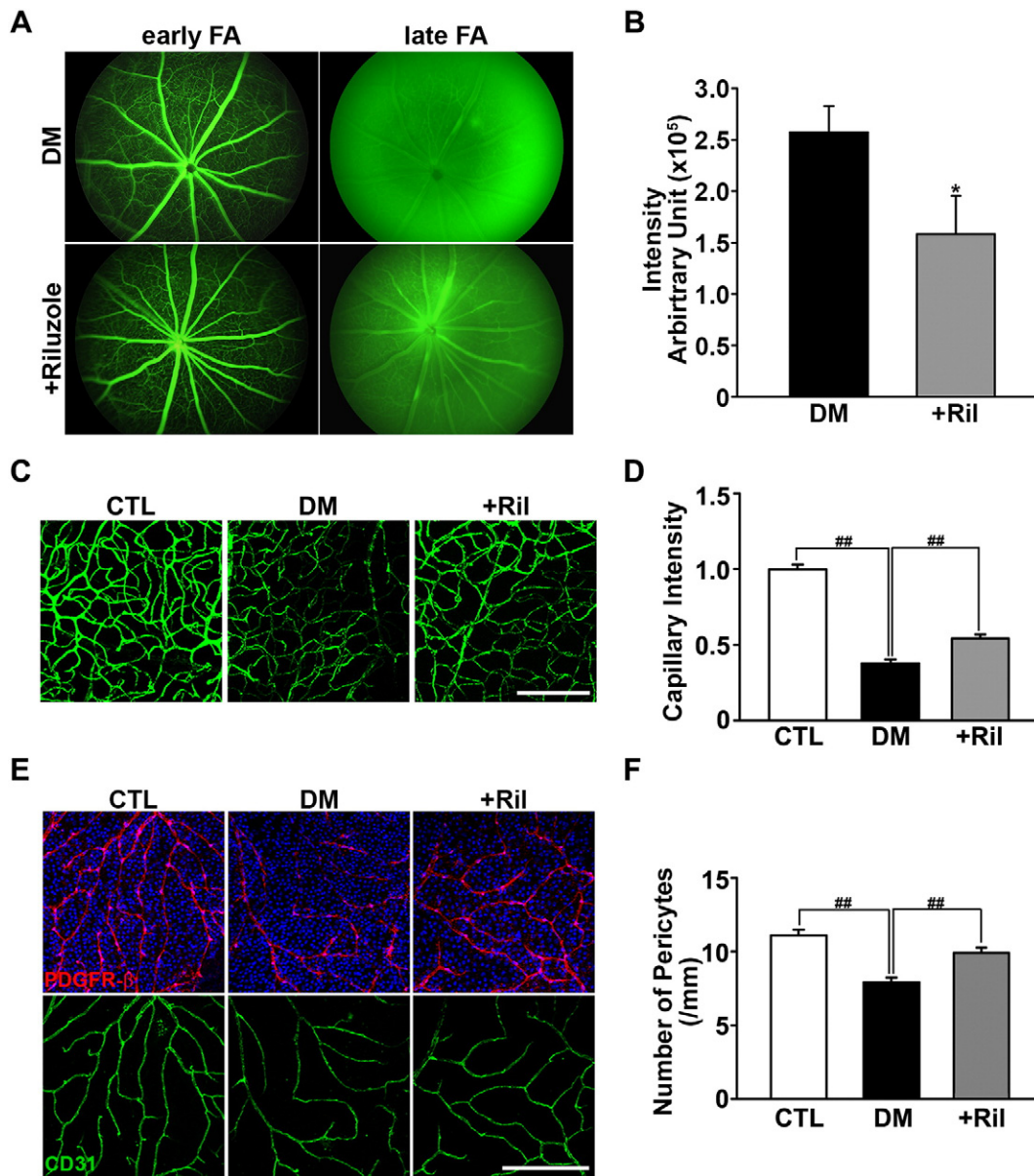


Fig. 6. Attenuation of DR by riluzole. (A) Representative photographs of fluorescein angiography taken 8 weeks after STZ injection showed attenuated fluorescein leakage at late stage in riluzole-treated diabetic mice ($n = 10$) compared to untreated diabetic mice ($n = 14$). (B) Quantification of fluorescein angiography results ($*P < 0.05$). (C) Perfusion was improved in DR by treatment with riluzole (green: FITC-dextran). (D) Quantification of capillary intensity ($##P < 0.001$). (E) Immunostaining of retinal flat mounts with antibodies for PDGFR- β (red), CD31 (green) and Hoechst (blue). Pericyte loss in DR was inhibited in riluzole-treated diabetic mice ($n = 6$) compared to untreated diabetic mice ($n = 6$). (F) Quantification of pericytes number ($##P < 0.001$). Original magnification, $\times 200$; scale bar, 200 μm .

confirmed this in vivo observation. Again, riluzole attenuated the loss of PDGFR- β -positive pericytes and ameliorated the reduction in perfusion.

Although experiments in whole cells suggest that riluzole is an effective PKC inhibitor, they do not address whether riluzole inhibits PKC directly or indirectly. To test the possibility that riluzole directly binds to PKC, we conducted docking simulations of riluzole in the ATP-binding site of PKC. A detailed binding-mode analysis indicated that riluzole binding in this site was facilitated by the formation of two hydrogen bonds with the backbone group in the hinge region and the side chain in the Gly loop. Simultaneously, van der Waals interactions with the nonpolar residues around the ATP-binding pocket were also found to contribute significant binding forces to the stabilization of the PKC-riluzole complex. These computational results strongly suggest that riluzole fits well into the ATP-binding site of PKC β , and argue that the attenuation of MCP1 induction and protection against retinal pericyte loss

in diabetic mice produced by riluzole is attributable to direct inhibition of PKC.

Collectively, the results of the present study demonstrate that riluzole, acting as a PKC inhibitor, attenuates the induction of MCP1 by AGE or mLDL in cultured retinal pericytes as well as in the STZ-induced mouse model of DR. These findings warrant further evaluation of the efficacy of riluzole in DR.

Supplementary data to this article can be found online at <http://dx.doi.org/10.1016/j.taap.2016.12.004>.

Conflict of interests

The authors declare no conflict of interests with respect to the research, authorship, and/or publication of this article.

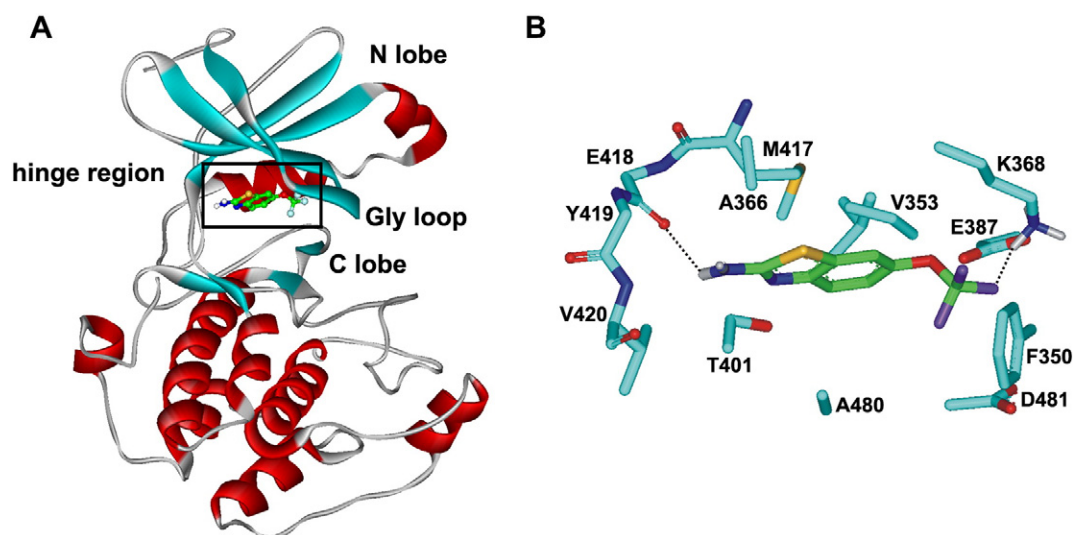


Fig. 7. Binding of riluzole to PKC β 3. (A) Docking pose of riluzole in the ATP-binding site of PKC. (B) Detailed binding mode of riluzole in the ATP-binding site of PKC. The carbon atoms of riluzole and PKC are shown in green and cyan, respectively. Hydrogen bonds are indicated with dotted lines.

Transparency document

The [Transparency document](#) associated with this article can be found, in the online version.

Acknowledgements

This study was supported by grants from the Ministry of Science, ICT and Future Planning, Republic of Korea: NRF-2013R1A2A2A01068457 and the Korea Health Technology R&D Project through the Korea Health Industry Development Institute (KHIDI): HI15C0527, HI14C1913.

Part of this study was presented as a poster at the 43rd Annual Meeting of the Society for Neuroscience, San Diego, California, 9–13 November 2013.

References

- Abcouwer, S.F., 2013. Angiogenic factors and cytokines in diabetic retinopathy. *J. Clin. Cell Immunol. (Suppl. 1)*, 1–12.
- Aiello, L.P., 2002. The potential role of PKC beta in diabetic retinopathy and macular edema. *Surv. Ophthalmol.* 47 (Suppl. 2), S263–S269.
- Bandello, F., Lattanzio, R., Zucchiatti, I., Del Turco, C., 2013. Pathophysiology and treatment of diabetic retinopathy. *Acta Diabetol.* 50, 1–20.
- Bhagat, N., Grigorian, R.A., Tutela, A., Zarbin, M.A., 2009. Diabetic macular edema: pathogenesis and treatment. *Surv. Ophthalmol.* 54, 1–32.
- Budhiraja, S., Singh, J., 2008. Protein kinase C beta inhibitors: a new therapeutic target for diabetic nephropathy and vascular complications. *Fundam. Clin. Pharmacol.* 22, 231–240.
- Cai, X., McGinnis, J.F., 2016. Diabetic retinopathy: animal models, therapies, and perspectives. *J. Diabetes Res.* 2016, 3789217.
- Chen, B.H., Jiang, D.Y., Tang, L.S., 2006. Advanced glycation end-products induce apoptosis involving the signaling pathways of oxidative stress in bovine retinal pericytes. *Life Sci.* 79, 1040–1048.
- Chew, E.Y., Davis, M.D., Danis, R.P., Lovato, J.F., Perdue, L.H., Greven, C., Genuth, S., Goff, D.C., Leiter, L.A., Ismail-Beigi, F., Ambrosius, W.T., 2014. The effects of medical management on the progression of diabetic retinopathy in persons with type 2 diabetes: the Action to Control Cardiovascular Risk in Diabetes (ACCORD) eye study. *Ophthalmology* 121, 2443–2451.
- Choi, J.A., Hwang, J.U., Yoon, Y.H., Koh, J.Y., 2013. Methallothionein-3 contributes to vascular endothelial growth factor induction in a mouse model of choroidal neovascularization. *Metallomics* 5, 1387–1396.
- Du, M., Wu, M., Fu, D., Yang, S., Chen, J., Wilson, K., Lyons, T.J., 2013. Effects of modified LDL and HDL on retinal pigment epithelial cells: a role in diabetic retinopathy? *Diabetologia* 56, 2318–2328.
- Eisma, J.H., Dulle, J.E., Fort, P.E., 2015. Current knowledge on diabetic retinopathy from human donor tissues. *World J. Diabetes* 6, 312–320.
- Friedman, E.A., 1999. Advanced glycosylated end products and hyperglycemia in the pathogenesis of diabetic complications. *Diabetes Care* 22 (Suppl. 2), B65–B71.
- Fu, D., Wu, M., Zhang, J., Du, M., Yang, S., Hammad, S.M., Wilson, K., Chen, J., Lyons, T.J., 2012. Mechanisms of modified LDL-induced pericyte loss and retinal injury in diabetic retinopathy. *Diabetologia* 55, 3128–3140.
- Gasteiger, J., Marsili, M., 1980. Iterative partial equalization of orbital electronegativity—a rapid access to atomic charges. *Tetrahedron* 36, 3219–3228.
- Geraldes, P., King, G.L., 2010. Activation of protein kinase C isoforms and its impact on diabetic complications. *Circ. Res.* 106, 1319–1331.
- Hammes, H.P., 2005. Pericytes and the pathogenesis of diabetic retinopathy. *Horm. Metab. Res.* 37 (Suppl. 1), 39–43.
- Jenkins, A.J., Velarde, V., Klein, R.L., Joyce, K.C., Phillips, K.D., Mayfield, R.K., Lyons, T.J., Jaffa, A.A., 2000. Native and modified LDL activate extracellular signal-regulated kinases in mesangial cells. *Diabetes* 49, 2160–2169.
- Kaur, C., Foulds, W.S., Ling, E.A., 2008. Blood-retinal barrier in hypoxic ischaemic conditions: basic concepts, clinical features and management. *Prog. Retin. Eye Res.* 27, 622–647.
- Kim, J.E., Kim, D.S., Kwak, S.E., Choi, H.C., Song, H.K., Choi, S.Y., Kwon, O.S., Kim, Y.I., Kang, T.C., 2007. Anti-glutamatergic effect of riluzole: comparison with valproic acid. *Neuroscience* 147, 136–145.
- Kim, Y.H., Kim, Y.S., Roh, G.S., Choi, W.S., Cho, G.J., 2012. Resveratrol blocks diabetes-induced early vascular lesions and vascular endothelial growth factor induction in mouse retinas. *Acta Ophthalmol.* 90, e31–e37.
- Koya, D., 2014. Dual protein kinase C alpha and beta inhibitors and diabetic kidney disease: a revisited therapeutic target for future clinical trials. *J. Diabetes Investig.* 5, 147–148.
- Lai, A.K., Lo, A.C., 2013. Animal models of diabetic retinopathy: summary and comparison. *J. Diabetes Res.* 2013, 106594.
- LeCaire, T.J., Palta, M., Klein, R., Klein, B.E., Cruickshanks, K.J., 2013. Assessing progress in retinopathy outcomes in type 1 diabetes: comparing findings from the Wisconsin Diabetes Registry Study and the Wisconsin Epidemiologic Study of Diabetic Retinopathy. *Diabetes Care* 36, 631–637.
- Leskova, W., Watts, M.N., Carter, P.R., Eshaq, R.S., Harris, N.R., 2013. Measurement of retinal blood flow rate in diabetic rats: disparity between techniques due to redistribution of flow. *Invest. Ophthalmol. Vis. Sci.* 54, 2992–2999.
- Lutty, G.A., 2013. Effects of diabetes on the eye. *Invest. Ophthalmol. Vis. Sci.* 54, ORSF81–ORSF87.
- Lyons, T.J., Li, W., Wojciechowski, B., Wells-Knecht, M.C., Wells-Knecht, K.J., Jenkins, A.J., 2000. Aminoguanidine and the effects of modified LDL on cultured retinal capillary cells. *Invest. Ophthalmol. Vis. Sci.* 41, 1176–1180.
- Menne, J., Shushakova, N., Bartels, J., Kiyan, Y., Laudeley, R., Haller, H., Park, J.K., Meier, M., 2013. Dual inhibition of classical protein kinase C- α and protein kinase C- β isoforms protects against experimental murine diabetic nephropathy. *Diabetes* 62, 1167–1174.
- Morris, G.M., Goodsell, D.S., Halliday, R.S., Huey, R., Hart, W.E., Belew, R.K., Olson, A.J., 1998. Automated docking using a Lamarckian genetic algorithm and an empirical binding free energy function. *J. Comput. Chem.* 19, 1639–1662.
- Motiejunaite, R., Kazlauskas, A., 2008. Pericytes and ocular diseases. *Exp. Eye Res.* 86, 171–177.
- Murakami, T., Frey, T., Lin, C., Antonetti, D.A., 2012. Protein kinase C beta phosphorylates occludin regulating tight junction trafficking in vascular endothelial growth factor-induced permeability in vivo. *Diabetes* 61, 1573–1583.
- Noh, K.M., Hwang, J.Y., Shin, H.C., Koh, J.Y., 2000. A novel neuroprotective mechanism of riluzole: direct inhibition of protein kinase C. *Neurobiol. Dis.* 7, 375–383.
- Panee, J., 2012. Monocyte Chemoattractant Protein 1 (MCP-1) in obesity and diabetes. *Cytokine* 60, 1–12.

- Praidou, A., Androudi, S., Brazitikos, P., Karakiulakis, G., Papakonstantinou, E., Dimitrakos, S., 2010. Angiogenic growth factors and their inhibitors in diabetic retinopathy. *Curr. Diabetes Rev.* 6, 304–312.
- Renier, G., Mamputu, J.C., Desfaits, A.C., Serri, O., 2003. Monocyte adhesion in diabetic angiopathy: effects of free-radical scavenging. *J. Diabetes Complicat.* 17, 20–29.
- Ruta, L.M., Magliano, D.J., Lemesurier, R., Taylor, H.R., Zimmet, P.Z., Shaw, J.E., 2013. Prevalence of diabetic retinopathy in Type 2 diabetes in developing and developed countries. *Diabet. Med.* 30, 387–398.
- Sims, D.E., 1986. The pericyte—a review. *Tissue Cell* 18, 153–174.
- Singh, V.P., Bali, A., Singh, N., Jaggi, A.S., 2014. Advanced glycation end products and diabetic complications. *Korean J. Physiol. Pharmacol.* 18, 1–14.
- Sonoki, K., Yoshinari, M., Iwase, M., Iino, K., Ichikawa, K., Ohdo, S., Higuchi, S., Iida, M., 2002. Glycoxidized low-density lipoprotein enhances monocyte chemoattractant protein-1 mRNA expression in human umbilical vein endothelial cells: relation to lysophosphatidylcholine contents and inhibition by nitric oxide donor. *Metabolism* 51, 1135–1142.
- Tarr, J.M., Kaul, K., Chopra, M., Kohner, E.M., Chibber, R., 2013. Pathophysiology of diabetic retinopathy. *ISRN Ophthalmol.* 2013, 343560.
- Thallas-Bonke, V., Thorpe, S.R., Coughlan, M.T., Fukami, K., Yap, F.Y., Sourris, K.C., Penfold, S.A., Bach, L.A., Cooper, M.E., Forbes, J.M., 2008. Inhibition of NADPH oxidase prevents advanced glycation end product-mediated damage in diabetic nephropathy through a protein kinase C- α -dependent pathway. *Diabetes* 57, 460–469.
- Trost, A., Lange, S., Schroedel, F., Bruckner, D., Motloch, K.A., Bogner, B., Kaser-Eichberger, A., Strohmaier, C., Runge, C., Aigner, L., Rivera, F.J., Reitsamer, H.A., 2016. Brain and retinal pericytes: origin, function and role. *Front. Cell. Neurosci.* 10, 20.
- Wagner, J., von Matt, P., Sedrani, R., Albert, R., Cooke, N., Ehrhardt, C., Geiser, M., Rummel, G., Stark, W., Strauss, A., Cowan-Jacob, S.W., Beerli, C., Weckbecker, G., Evenou, J.P., Zenke, G., Cottens, S., 2009. Discovery of 3-(1H-indol-3-yl)-4-[2-(4-methylpiperazin-1-yl)quinazolin-4-yl]pyrrole-2,5-dione (AEB071), a potent and selective inhibitor of protein kinase C isotypes. *J. Med. Chem.* 52, 6193–6196.
- Williams, R., Airey, M., Baxter, H., Forrester, J., Kennedy-Martin, T., Girach, A., 2004. Epidemiology of diabetic retinopathy and macular oedema: a systematic review. *Eye (Lond.)* 18, 963–983.
- Witmer, A.N., Vrensen, G.F., Van Noorden, C.J., Schlingemann, R.O., 2003. Vascular endothelial growth factors and angiogenesis in eye disease. *Prog. Retin. Eye Res.* 22, 1–29.
- Wu, L., Fernandez-Loaiza, P., Sauma, J., Hernandez-Bogantes, E., Masis, M., 2013. Classification of diabetic retinopathy and diabetic macular edema. *World J. Diabetes* 4, 290–294.
- Yau, J.W., Rogers, S.L., Kawasaki, R., Lamoureux, E.L., Kowalski, J.W., Bek, T., Chen, S.J., Dekker, J.M., Fletcher, A., Grauslund, J., Haffner, S., Hamman, R.F., Ikram, M.K., Kayama, T., Klein, B.E., Klein, R., Krishnaiah, S., Mayurasakorn, K., O'Hare, J.P., Orchard, T.J., Porta, M., Rema, M., Roy, M.S., Sharma, T., Shaw, J., Taylor, H., Tielsch, J.M., Varma, R., Wang, J.J., Wang, N., West, S., Xu, L., Yasuda, M., Zhang, X., Mitchell, P., Wong, T.Y., 2012. Global prevalence and major risk factors of diabetic retinopathy. *Diabetes Care* 35, 556–564.
- Zhang, S.X., Wang, J.J., Dashti, A., Wilson, K., Zou, M.H., Szweida, L., Ma, J.X., Lyons, T.J., 2008. Pigment epithelium-derived factor mitigates inflammation and oxidative stress in retinal pericytes exposed to oxidized low-density lipoprotein. *J. Mol. Endocrinol.* 41, 135–143.